HHS Public Access

Author manuscript

J Comp Neurol. Author manuscript; available in PMC 2019 August 01.

Published in final edited form as:

J Comp Neurol. 2018 August 01; 526(11): 1790–1805. doi:10.1002/cne.24448.

GABA-like Immunoreactivity in *Biomphalaria*: Colocalization with Tyrosine Hydroxylase-like Immunoreactivity in the Feeding Motor Systems of Panpulmonate Snails

Lee O. Vaasjo[1], **Alexandra M. Quintana**[1], **Mohamed R. Habib**[2], **Paola A. Mendez de Jesus**[1], **Roger P. Croll**[3], and **Mark W. Miller**[1]

[1]Institute of Neurobiology and Department of Anatomy & Neurobiology, University of Puerto Rico, Medical Sciences Campus, San Juan, Puerto Rico

[2]Medical Malacology Laboratory, Theodor Bilharz Research Institute, Giza, Egypt

[3]Department of Physiology and Biophysics, Dalhousie University, Halifax, Nova Scotia, Canada

Abstract

The simpler nervous systems of certain invertebrates provide opportunities to examine colocalized classical neurotransmitters in the context of identified neurons and well defined neural circuits. This study examined the distribution of γ-aminobutyric acid-like immunoreactivity (GABAli) in the nervous system of the panpulmonates *Biomphalaria glabrata* and *Biomphalaria alexandrina*, major intermediate hosts for intestinal schistosomiasis. GABAli neurons were localized in the cerebral, pedal, and buccal ganglia of each species. With the exception of a projection to the base of the tentacle, GABAli fibers were confined to the CNS. As GABAli was previously reported to be colocalized with markers for dopamine (DA) in five neurons in the feeding network of the euopisthobranch gastropod *Aplysia californica* (Díaz-Ríos et al. 2002), double-labeling protocols were used to compare the distribution of GABAli with tyrosine hydroxylase immunoreactivity (THli). As in *Aplysia*, GABAli-THli colocalization was limited to five neurons, all of which were located in the buccal ganglion. Five GABAli-THli cells were also observed in the buccal ganglia of two other intensively studied panpulmonate species, *Lymnaea stagnalis* and *Helisoma trivolvis*. These findings indicate that colocalization of the classical neurotransmitters GABA and DA in feeding central pattern generator (CPG) interneurons preceded the divergence of euopisthobranch and panpulmonate taxa. These observations also support the hypothesis that heterogastropod feeding CPG networks exhibit a common universal design.

Graphical Abstract

GABA-like immunoreactivity (magenta) and tyrosine hydroxylase-like immunoreactivity (green) in the anterolateral quadrant of the cerebral ganglion of the pulmonate snail, *Biomphalaria glabrata*. Species of *Biomphalaria* are the major intermediate hosts for *Schistosoma mansoni*, the trematode worm that causes the most widespread from of schistosomiasis.

*Address for correspondence: Dr. Mark W. Miller, Institute of Neurobiology, 201 Blvd del Valle, San Juan, Puerto Rico 00901, Tel: 1.787.721.1237, Fax: 1.787.725.3804, mark.miller@upr.edu.

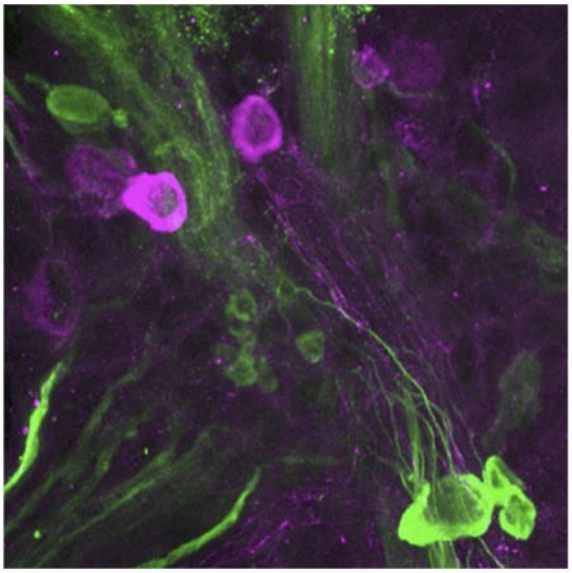

Keywords

RRID:AB 477652: Rabbit Anti-GABA Antibody; Unconjugated; Sigma-Aldrich; RRID:AB_572268: Tyrosine Hydroxylase Antibody; ImmunoStar; schistosomiasis; dopamine; γ-aminobutyric acid; catecholamines; *Biomphalaria glabrata*; *Helisoma trivolvis*; *Lymnaea stagnalis*; *Biomphalaria alexandrina*

Introduction

Increasing evidence supports the hypothesis that classical neurotransmitters can be colocalized in individual neurons (Seal and Edwards 2006: Gutíerrez 2009; Borisovska and Westbrook 2014; Vaaga et al. 2014). One such combination, γ–aminobutyric acid (GABA) with dopamine (DA), has been reported in several cell types within in vertebrate nervous systems, including periglomerular cells of the mouse olfactory bulb (Maher and Westbrook 2008; Borisovska et al. 2013; Liu et al. 2013), retinal amacrine cells (Hirasawa et al. 2009, 2015), mouse nigrostriatal and ventral tegmental cells (Tritsch et al. 2012, 2016; Trudeau et al. 2014), nerve terminals of the *Xenopus laevis* pituitary (de Rijk et al. 1992), and neurons in the spinal cord of the sea lamprey (Barreiro-Iglesias et al. 2009). While proposed mechanisms of release from GABA-DA neurons range from independent nonsynaptic volume transmission in the retina to co-release from shared synaptic vesicles in the striatum, much remains unknown about the functional consequences of this neuronal phenotype and its occurrence across phylogeny (Kim et al. 2015). It has been proposed the simpler nervous systems of certain invertebrates can provide opportunities to further examine colocalized classical neurotransmitters in the context of identified neurons and defined neural circuits (Miller 2009).

In gastropod molluscs, a neurotransmitter role for GABA was initially suggested by pharmacological studies in which it was found to produce both excitatory and inhibitory responses upon application to snail neurons (Gerschenfeld and Tauc 1961; Walker et al.

1971, 1975). Biochemical approaches demonstrated the presence of GABA, its synthesis, and its uptake in the central nervous systems of several gastropod species (Osborne et al. 1971; Dolezalova et al. 1973; Cottrell 1977). The localization of GABA to specific neurons within gastropod nervous systems was demonstrated with autoradiographic and immunohistological techniques in *Planorbis* (Turner and Cottrell 1978), *Limax* (Cooke and Gelperin 1988), *Helisoma* (Richmond et al. 1991), *Clione* (Arshavsky et al. 1993, Norekian 1999), *Helix* (Hernadi 1994), *Aplysia* (Díaz-Ríos et al. 1999), *Pleurobranchaea*, and four nudibranchs species (Gunaratne et al. 2014, Gunaratne and Katz 2016).

DA is also well established as major neurotransmitter in the gastropod central nervous system where it, like GABA, can produce both excitatory and inhibitory synaptic actions (Sweeney 1963; Osborne and Cottrell 1971; Ascher 1972; Berry and Cottrell 1973; McCaman et al. 1979). Early studies exploited aldehyde- or glyoxylate- induced fluorescence techniques to demonstrate the presence of catecholamine-containing neurons in both the central nervous system and periphery of several species (Tritt et al. 1983; Salimova et al. 1987a, b; Croll 1988; Croll et al. 1999). Biochemical analyses also demonstrated significant levels of catecholamines, particularly dopamine, within the nervous system of several gastropods (McCaman et al. 1973; McCaman 1984; Walker 1986; Croll et al. 1999). More recently, immunohistochemical localization of tyrosine hydroxylase (TH), the rate-limiting enzyme in catecholamine biosynthesis, was shown to label neurons that utilize DA as a neurotransmitter in gastropods (Croll et al. 1999; Croll 2001).

In addition to their individual roles as gastropod neurotransmitters, evidence suggests that GABA and DA may co-exist in specific neurons in the euopisthobranch gastropod *Aplysia californica* (Díaz-Ríos et al. 2002). The colocalization of GABA and DA in five identified neurons within the feeding central pattern generator circuit of *Aplysia* enabled investigators to probe their respective contributions to synaptic signaling and specification of motor patterns in a multifunctional motor system (Due et al. 2004; Díaz-Ríos and Miller 2005, 2006; Svensson et al. 2014).

The present study was designed with three objectives: 1) We first mapped the distribution of GABA like immunoreactivity (li) in the nervous systems of two species of panpulmonate snails, *Biomphalaria glabrata* and *Biomphalaria alexandrina*. In previous studies, we fully mapped the localization of catecholamines in the nervous systems of these species (Vallejo et al. 2014) and showed that TH provided a reliable means of labeling neurons that utilize DA as a neurotransmitter (Vallejo et al. 2014). This work is part of our investigation of neurotransmitters in intermediate snail hosts for larval trematodes that cause the tropical disease schistosomiasis (see also Delgado et al. 2012; Habib et al. 2015; Mansour et al. 2017). 2) With complete maps of putative, GABAergic and dopaminergic neurons in place, we next directly assessed the prospect of GABA-DA colocalization in *B. glabrata* using double labelling immunohistochemical techniques. 3) Finally, we also examined colocalization of GABA and THli in the feeding motor systems of *Lymnaea stagnalis* and *Helisoma trivolvis*, two panpulmonate species in which the neural control of feeding has been intensively studied.

Materials and Methods

Immunohistochemistry

Mature specimens (8–10 mm shell diameter) of *Biomphalaria glabrata, Biomphalaria alexandrina* and *Helisoma trivolvis* and juvenile specimens of *Lymnaea stagnalis* (also 8–10 mm shell length) were dissected in Petri dishes lined with Sylgard (Dow Chemical) and containing pond snail saline (see Delgado et al. 2012). *Biomphalaria* and *Lymnaea* ganglia were incubated in 0.5% protease type XIV (Sigma-Aldrich, St. Louis MO; Product #P5147) for 8–10 min at room temperature. Following washes (5x, 10–20 min) with snail saline, *Biomphalaria* and *Lymnaea* ganglia were fixed with 4% paraformaldehyde (4° C, 1 h). They were then treated with a heat-induced epitope retrieval (HIER) protocol (Abcam IHC antigen retrieval protocol). Samples were incubated in a heated (60° C, 30 min) sodium citrate buffer (10 mM trisodium citrate dihydrate [Sigma-Aldrich], 0.05% Tween 20 [Fisher Scientific], pH 6.0). *Helisoma* tissues were fixed overnight in Zamboni's fixative (125 ml of 16% paraformaldehyde, 150 ml saturated picric acid solution per liter phosphate buffer, pH 7.3). They were not treated with protease and were not subjected to the HIER protocol.

For peripheral tissues, protocols were used as described previously (Habib et al., 2015). Tissues were incubated in .25% collagenase IV (Sigma-Aldrich, Product #C-5138) for 2–3 h, then placed between two glass slides spaced apart with a small piece of modeling clay, incubated at 4° C for 25–30 minutes and then fixed for 1 h by perfusing 4% paraformaldehyde between the slides. To remove the fixative, tissues were removed from between the slides, placed in microcentrifuge tubes and washed (5x, 30 min) with 0.5% PBS-T (PBS-T: 0.2 M PBS buffer, 0.5% Triton X-100).

GABAli was detected with a polyclonal rabbit antibody (RRID Sigma-Aldrich, Product #A2052) generated against GABA conjugated to bovine serum albumin (BSA). Dot blots showed that this antibody recognizes GABA and not BSA (Sigma-Aldrich data sheet). In gastropods, neurons labeled with this antibody have been shown to produce GABAergic synaptic signals (Jing et al. 2003; Wu et al. 2003). Catecholaminergic neurons were detected with a mouse monoclonal antibody (RRID: Immunostar, Stillwater MN; product No. 22941) generated against rat tyrosine hydroxylase [lot LNC1 purified from rat pheochromocytoma (PC12) cells]. This antibody is reported to possess wide species cross-reactivity, due to its recognition of a highly conserved epitope in the midportion of the TH molecule (Immunostar specification sheet 22914). It specifically labels neurons that are stained with several independent catecholaminergic markers, including the glyoxylic acid (Rathouz and Kirk 1988; Kabotyanski et al. 1998) and the formaldehyde (Fa)-glutaraldehyde (Glu) histofluorescent techniques (Goldstein and Schwartz 1989; Croll 2001; Díaz-Ríos et al. 2002). We previously reported that synaptic signals produced by neurons labeled with this antibody in *B. glabrata* were blocked by the dopamine antagonist sulpiride (Vallejo et al. 2014). Tissues of all species were incubated in a solution containing both primary antibodies (TH: 1:100; GABA: 1:200) diluted in PBS-Tx (0.25% Triton X-100, 1% Bovine Serum Albumin V (IgG free), 2% normal goat serum, 1% dimethyl sulfoxide in 0.2 M PBS) at 4° C for 5 days (Gunaratne et al. 2014; Vallejo et al. 2014). Antibody dilutions were based upon prior reports for wholemount immunohistochemistry of gastropod ganglia (Díaz Ríos et al.

1999; Croll 2001; Díaz Ríos and Miller 2002; Vallejo et al. 2014; Gunaratne and Katz 2016). Following repeated PBS-T washes (5x, 20 min, room temperature), tissues were incubated in the dark in second antibodies conjugated to fluorescent markers (Alexa 488 goat anti-mouse IgG (H+L) conjugate; Molecular Probes and Alexa 546 goat anti-rabbit IgG (H+L) conjugate; Molecular Probes). The second antibody dilutions ranged from 1:500 to 1:1,000. Following final PBS-T washes (5x, 20 min, room temperature) ganglia were placed in glycerol: PBS (6:1).

Laser scanning confocal image stacks of fluorescent immunohistochemical labeling were acquired on a Nikon A1R resonant scanning confocal microscope using 10x and 20x objectives. Some high magnification images were taken using the NIS Elements Nyquist sampling setting. Whole brain images were collected using a Tile scan at 3×2 and Stitching at 15%. Series of optical sections at 0.5–1.5 μm intervals were used to make maximum intensity projections and merged images using the open source ImageJ Java-based image processing and analysis program (National Institutes of Health; http://imagej.nih.gov/ij/). Plates were assembled and contrast adjustment of figures was implemented using Microsoft PowerPoint (v. 14.0, Microsoft Corp., Redmond, WA, USA). Schematic diagrams were created in Illustrator CS2 (Adobe Systems). Results reported in this study were observed in a minimum of 7 specimens of each species.

Protocols conducted on *B. glabrata* were approved by the Institutional Animal Care and Use Committee (IACUC) of the University of Puerto Rico Medical Sciences Campus (UPR-MSC; Protocol #3220110). Protocols conducted on *B. alexandrina* were approved by the Animal Care Committee of Dalhousie University (Protocol #I13-06). UPR-MSC IACUC protocol #3220109 was approved for the experiments conducted on *Helisoma trivolvis* and *Lymnaea stagnalis*.

Results

As no consistent differences were observed between the localization of GABA-like immunoreactivity in *B. glabrata* and *B. alexandrina*, the following description is applicable to both species. Double labeling experiments were performed on *B. glabrata* to compare the locations of GABA-immunoreactive cells and neurons that exhibit TH-like immunoreactivity (Fig. 1–7). In some cases, higher definition of GABAli cell structure was obtained in single labeling experiments on *B. alexandrina* (Fig. 1g–i).

Cerebral ganglion

On the dorsal surface of the cerebral ganglion, GABAli fibers were present in the tentacular nerve (*T n.*) and in four to six small neurons near the origin of the T n. (Fig. 1a, d, *arrows*). As reported by Vallejo et al. (2014), the T n. also contained a bundle of THli fibers that originated from small peripheral cells in the tentacle epithelium. The THli fiber bundle was more compact than the GABAli axons and occupied a distinct portion of the nerve (Fig. 1b, e). THli neurons were also observed near the origin of the T n. (Fig. 1b, e, *arrowheads*). Merged images of GABAli and THli did not reveal instances of colocalization on the dorsal surface of the cerebral ganglion (Fig. 1c, f).

Experiments were performed to trace the T n. GABAli fibers to the periphery (Fig. 1g–i). A loose bundle of axons projected to the epithelium at the base of the tentacle (Fig. 1g). The fibers were heterogeneous in diameter, with some having smooth contours and others *en passant* varicosities. They underwent extensive branching and terminated as varicose fibers below the surface of the epithelium at the base of the tentacle (Fig. 1h, i). It has been proposed that the major site of chemoreceptors for food detection in *Biomphalaria* is located in the body wall at the base of the tentacle, suggesting a role for GABA in processing sensory information (Townsend, 1974; see Discussion). No peripheral GABli cell bodies were detected and no GABAli fibers projected into the tentacle.

On the ventral surface of the cerebral ganglion, a dense network of GABAli fibers was located in the anterolateral region of each hemiganglion (Fig. 2a). Two to three small (10 – 20 μm) GABAli neurons (Fig. 2d, *arrowheads*) were observed near the origin of the cerebral-buccal connective (see also Fig. 2g). Four to five GABAli fibers were present in each cerebral-buccal connective (C-b c.) and in the cerebral commissure (C c.). No GABAli fibers were detected in the medial lip nerve (Fig. 2d–f, M Lip n.), the lateral lip nerve (Fig. 2d–f, L Lip n.), or the penis nerve.

A previous study showed that prominent THli fiber systems in the lip nerves originate predominantly from peripheral neurons (Vallejo et al. 2014). A group of THli central neurons was observed in the anterolateral region the cerebral ganglion, however (Fig. 2e, h, *arrowheads)*, prompting double-labeling experiments to test for the presence of GABA-TH colocalization. Merged images of GABAli and THli did not reveal instances of colocalization (Fig. 2c, f, i).

Pedal ganglion

Two tightly apposed GABAli cell bodies were positioned on the dorsal surface of the left pedal ganglion between the origin of the anterior pedal nerve and the pedal commissure (Fig. 3a, inset). The larger (25 – 30 μm) of these cells, termed LPeD2, was the largest GABAli neuron in the entire CNS. It was located in a slightly more lateral position than its smaller (15 – 20 μm) neighbor. LPeD2 gave rise to a large axon that coursed in a posterolateral direction toward the pedal-pleural connective, medial to the axon of the giant dopaminergic cell LPeD1 (Vallejo et al. 2014; Fig. 3a–c, d–f).

A cluster of four smaller (10 – 15 μm) posterolateral GABAli neurons was located near the axon of LPeD2 (Fig. 3a, d, *arrowheads).* A similar cluster was observed in the right pedal ganglion near the confluence of the central pedal nerve and the pedal-pleural connective (Fig. 3a, g, *arrowheads*). A second group of small (10 – 15 μm) GABAli neurons was present in the right pedal ganglion near the origin of the anterior pedal nerve (Fig. 3a, g, *arrows*). No GABAli fibers were detected in the pedal nerves.

In a prior report, small THli neurons were observed in the dorsolateral regions of the pedal ganglion near the origins of the pedal nerves (Vallejo et al. 2014). Preparations that were labeled for GABAli (Fig. 3a, d, g) were therefore processed for THli (Fig. 3b, e, h) in order to determine the relative positions of these two systems and to test for their colocalization. Single THli neurons were located near both posterolateral GABAli clusters (Fig. 3i,

arrowhead) and within the cluster at the base of the anterior pedal nerve (Fig. 3i, *arrow*), but in no case was THli colocalized with GABAli.

On the ventral surface of the pedal ganglia, clusters of small (10 – 15 μm) GABAli neurons were observed lateral to the origin of each posterior pedal nerve (Fig. 4a, d, g, *arrows*). While similar groups of THli cells were located in close proximity (Fig. 4b, e, h, *arrowheads*), no instances of colocalization were detected when images of GABAli and THli were merged (Fig. 4c, f, i).

Pleural, Parietal, and Visceral Ganglia

No GABAli cells were detected in the pleural, parietal, or visceral ganglia of *B. glabrata*. A rich network of GABAli fibers coursed through the pleural and parietal ganglia, giving rise to fine branches and terminals (Fig. 5a). While several THli fibers were also observed, they did not exhibit extensive branching (Fig. 5b). When images of GABAli and THli were merged (Fig. 5c), the THli fibers appeared to occupy more lateral positions and no clear instances of colocalization were detected. Several large THli fibers projected to the parietal nerves and a few fine GABAergic axons terminated in the initial segments of these nerves.

GABAli fibers and terminals were present throughout the central regions of the visceral and left parietal ganglia (Fig. 5d). The THli systems in these ganglia exhibited less branching (Fig. 5e). While several THli fibers projected to the peripheral nerves, the GABAli system was confined to the CNS (Fig. 5f). No evidence for GABAli-THli colocalization was detected.

Buccal Ganglion

A prominent system of GABAli fibers coursed through the core of the buccal ganglion (Fig. 6a). Large caliber fibers were present in the cerebral-buccal connective and crossing the buccal commissure. No GABAli fibers were present in the buccal nerves.

A single GABAli neuron was located on the ventral surface of each buccal hemiganglion (Fig. 6a, d). A fiber projected from each cell in the medial direction joining the central GABAli neuropil. When preparations were processed for THli, only two ventral neurons were labeled (Fig. 6b, e; see also Vallejo et al. 2014). Merging the images for GABAli and THli showed that they were labeling the same cells (Fig. 6c, f).

Five to seven GABAli neurons were dispersed across the dorsal surface of each buccal hemiganglion (Fig. 7a). While labeling of the two hemiganglia was generally symmetrical, one buccal GABAli neuron was only present in the right hemiganglion, adjacent to the buccal commissure (Fig. 7a, *arrow*). When THli was compared to GABAli, colocalization was observed in the unpaired cell (Fig. 7b,c,e,f, *arrows*) and in one lateral neuron near the origin of the C-b c. (Fig. 7b,c,e,f, *arrowheads*).

Buccal ganglia of *Lymnaea stagnalis* and *Helisoma trivolvis*

The limited occurrence of GABAli –THli colocalization in five buccal ganglion neurons in *B. glabrata* was in agreement with our previous observations in the marine euopisthobranch *Aplysia californica* (Díaz-Ríos et al. 2002; Díaz-Ríos and Miller 2005, 2006). It was

therefore of interest to examine whether this pattern of colocalization was also present in the buccal ganglia of other panpulmonate species in which the feeding central pattern generators have been intensively studied.

In *Lymnaea stagnalis*, a single GABAli neuron was located on the ventral surface of each buccal hemiganglion (Fig. 8a, d). THli was also observed in only two ventral cells (Fig. 8b, e). Merging the images for GABAli and THli showed that both protocols were labeling the same pair of cells (Fig. 8c, f). The ventral GABAli – THli cells of *Lymnaea* were located in a similar position as those of *Biomphalaria*, slightly posterior to the central fiber system. As observed with the ventral GABAli – THli cells of *B. glabrata* (Fig. 6), a fiber projected in the anteromedial direction toward the buccal commissure (Fig. 8d–f, *arrows*).

Another four to six GABAli cells were labeled on the dorsal surface of each *Lymnaea* buccal hemiganglion (Fig. 9a). Most of the dorsal GABAli cells were located in the lateral portion of the ganglion, near the confluence of the C-b c. and the dorsobuccal nerve (Db n.). However, one medial unpaired GABAli neuron was present in the left hemiganglion adjacent to the buccal commissure (Fig. 9a, *arrow*). When ganglia were processed for THli, double-labeling was detected in one of the lateral GABAli neurons (Fig. 9a–3, *arrowheads*, 9d–f, *arrows*) and in the medial unpaired cell (Fig. 9a–c, *arrows*).

The colocalization of GABAli and THli was also observed in five neurons in the buccal ganglion of *Helisoma trivolvis* (Fig. 10). A bilateral pair of cells on the ventral surface was located near the fiber tract connecting the two hemiganglia (Fig. 10a–c; *arrows*). On the dorsal surface, GABAli and THli were colocalized in a pair of lateral neurons (Fig. 10d–f, *arrows*) and in an unpaired medial cell in the right hemiganglion (Fig. 10d–f, *arrowheads*). The medial GABA-THli neuron gave rise to two fibers that joined the central tract (Fig. 10g–i, *arrows*).

Discussion

GABA-like immunoreactivity in the CNS of *Biomphalaria* spp

The distributions of GABAli neurons in *B. glabrata* and *B. alexndrina* were indistinguishable (Fig. 11). GABAli cell bodies were limited to the cerebral, pedal, and buccal ganglia, in agreement with observations in other panpulmonate species, such as *Helix pomatia* (Hernádi 1994), *Helisoma trivolvis* (Richmond et al. 1991), and *Limax maximus* (Cooke and Gelperin 1988). A broader distribution, including cells in the parietal and visceral ganglia, was reported in *Lymnaea stagnalis* (Hatakeyama and Ito 2000).

The presence of GABAli fibers in each of the connectives joining the central ganglia suggests an involvement of GABAergic neurons in the coordination or specification of behavior in *Biomphalaria.* Two GABAergic cerebral-buccal interneurons (CBIs), termed CBI-12 and CBI-3, were identified in *Aplysia* (Euopisthobranchia, Anaspidea) and shown to exert specific GABA-mediated actions on the feeding CPG (Jing et al. 2003; Wu et al. 2003; see also Narusuye 2005). In *Clione limacina* (Euopisthobranchia, Pteropoda) a GABAergic CBI termed Cr-BM coordinates three motor programs that implement an elaborate carnivorous motor program (Norekian and Malyshev 2005). The presence of GABAli fibers

in the cerebral-buccal connective and GABAli cell bodies near the origin of the C-b c. indicates that similar higher order GABAergic control of feeding could operate in *Biomphalaria* and other panpulmonates.

The presence of major GABAergic tracts in the commissures of the cerebral, pedal, and buccal ganglia is consistent with observations in other panpulmonate species as well as in euopisthobranchs and nudibranchs (Cooke and Gelperin 1988; Richmond et al. 1991; Díaz-Ríos et al. 1999; Gunaratne et al. 2014, 2016). These paired ganglia control motor behaviors such as feeding and locomotion that require bilateral coordination. The participation of GABAergic signaling in maintaining bilateral coordination has been demonstrated in the buccal CPG of *Aplysia* where two GABAergic interneurons, B34 and B40, exert predominant synaptic actions in the contralateral buccal hemiganglion (Hurwitz et al. 1997; Jing et al. 2003). Interestingly, both B40 and B34 also project to the cerebral ganglion via the contralateral cerebral-buccal connective (Hurwitz et al. 1997; Jing et al. 2003). The presence of GABA in buccal-cerebral interneurons (BCIs) as well as CBIs (see above) indicates that this neurotransmitter system plays a bidirectional role in interganglionic signaling in the *Aplysia* feeding system. Further characterization of GABAergic CBIs and BCIs in the panpulmonates should increase our understanding of how this neurotransmitter system contributes to feedforward and feedback signaling between higher order regulatory elements and the feeding CPGs.

In addition to a GABAergic involvement in the central control of motor systems, the projection of fibers to the periphery via each tentacular nerve suggests a limited sensory function. The termination of this bundle in a region of the skin near the base of the tentacle is in agreement with previous studies in *Biomphalaria* that found the skin behind the origin of the tentacle to be highly sensitive to food application (Townsend 1974). As snails continued to orient toward applied food following ablation of the tentacles, this skin region was proposed to be the major chemoreceptive organ for food-finding. The tentacles were suggested to function mainly to guide chemostimulants to their base via ciliary currents (Townsend 1974). While pharmacological evidence supports a role for GABA in chemoreceptive function in pulmonates (Nezlin et al. 1997; Ito et al. 2004), GABAergic innervation of cephalic sensory organs has not been reported in other species.

GABAli-THli colocalization

Colocalization of GABAli and THli was previously observed in the euopisthobranch *Aplysia californica* (Díaz-Ríos et al. 2002). While GABAli and THli neurons were present throughout the central nervous system of *Aplysia*, their colocalization was limited to five neurons in the paired buccal ganglia. The present study surveyed the distribution of GABAli *Biomphalaria glabrata*, *Helisoma trivolvis*, and *Lymnaea stagnalis* and found that colocalized GABAli and THli was similarly limited to five buccal neurons. In *Aplysia*, GABAli-THli colocalization occurs in two identified pairs of interneurons, termed B20 and B65. Similar to the GABAergic neurons B34 and B40 described above, B65 is a dorsal cell that projects to the cerebral ganglion via the contralateral C-b connective. B20 is a bipolar ventral cell that projects to both C-b connectives. To the extent that their anatomy can be determined from our experiments, the positions, shapes, and projections of the GABAli –

THli cells observed in the panpulmonates are highly similar to the morphological properties of the GABA-DA neurons in *Aplysia*.

B20 and B65 are capable of initiating coordinated buccal motor patterns (Kabotyanski et al. 1998; Teyke et al. 1993). Moreover, each is thought to play a critical role in determining the functional output of the feeding CPG (Kabotyanski et al. 1998; Jing and Weiss 2001; Proekt et al. 2004; Due et al. 2004). Rapid excitatory postsynaptic potentials (EPSPs) produced by both B65 and B20 in buccal motor neuron targets were occluded by dopamine, but not GABA, and blocked by the dopamine antagonist sulpiride (Due et al. 2004; Díaz-Ríos and Miller 2005). It was therefore proposed that these rapid EPSPs were mediated by dopamine. GABA, acting through GABAB-like receptors and protein kinase C, was shown to modulate the rapid dopaminergic EPSPs in a target specific manner (Díaz-Ríos and Miller 2005, 2006; Svensson et al. 2014). The comprehensive understanding of the anatomy, physiology, and function of B20 and B65 provides a contextual framework for characterizing the GABA-DA phenotype in panpulmonates.

To date, the unpaired GABAli –THli neuron in the *Aplysia* buccal system remains unidentified. Unpaired buccal cells have been characterized in gastropod buccal systems, including the 'slow oscillator' (SO) neuron of *Lymnaea* (Elliott and Benjamin 1985) and B50 in *Aplysia* (Dembrow et al. 2003). The medial bipolar unpaired GABAli-THli cells observed here in the panpulmonates are unlikely to correspond to SO or B50 which are located in the lateral region of the ganglion and project a single process that crosses the buccal commissure. Moreover, pharmacological evidence indicates that SO and B50 are both cholinergic. It is noteworthy that the unpaired cell soma in the pulmonates examined here was located in the right hemiganglion of the sinistral species *Biomphalaria* and *Helisoma* and in the left hemiganglion of the dextral species *Lymnaea*.

Implications for a Conserved Feeding Central Pattern Generator in Gastropods

The motor circuits that generate feeding in gastropods have been intensively studied in species that employ highly diverse ingestive behaviors (e.g. Kupfermann 1974; Arshavsky et al. 1991; Benjamin et al. 2000). Comparative studies of gastropod feeding networks can thus provide insight into circuit elements that are conserved and those that are modified to adapt to changing demands (Murphy 2001; Elliott and Susswein 2002; see Paul 1991; Katz and Harris-Warrick 1999).

Murphy (2001) advanced the 'universal tripartite model' for the feeding central pattern generator circuits of gastropod molluscs, and proposed homology between specific core interneurons in several species (see also Wentzell et al. 2009). Among the proposed homologies, the B20 and B65 neurons of *Aplysia* were hypothesized to correspond to identified neurons in the panpulmonates *Lymnaea stagnalis* and *Helisoma trivolvis* (Murphy 2001). These homologies were based upon cell location, morphology, synaptic connections, CPG function, and dopaminergic phenotype. The present study adds GABA-like immunoreactivity to these shared features and supports the notion of a common CPG core underlying highly variable gastropod feeding behaviors.

The presence of five GABAli-THli neurons in the feeding networks of three panpulmonate species suggests that this colocalization predates the divergence of the euopisthobranch and panpulmonate groups. Molecular clock analysis estimates that this divergence occurred approximately 237 Mya near the Permian/Triassic transition. The recent localization of GABAli in the buccal ganglia of Nudipleura (Gunaratne et al. 2016) sets the stage for exploring whether GABA-DA colocalization predated divergence of the Tectipleura and Nudipleura groups. This avenue of investigation should provide opportunities to explore the functional consequences of classical neurotransmitter colocalization in identified neurons and tractable motor networks (Miller 2009). This approach should also inform our understanding of cotransmission by classical neurotransmitters in more complex vertebrate nervous systems.

Acknowledgments

National Institutes of Health: RCMI MD007600, MBRS GM087200; National Science Foundation: DBI-1337284, HRD-1137725, OISE 1545803; National Academy of Sciences (NAS; USA) U.S.-Egypt Science and Technology (S&T) Joint Fund 2000007152*; Science and Technology Development Fund (STDF, Egypt): USC17-188; Natural Sciences and Research Council (Canada): Discovery Grant 38863.

References

Arshavsky YI, Gamkrelidze GN, Orlovsky GN, Panchin YV, Popova LB. Gamma-aminobutyric acid induces feeding in the pteropod mollusk *Clione limacina*. Neuroreport. 1991; 2:169–172. [PubMed: 1893089]

Arshavsky YI, Deliagina TG, Gamkrelidze GN, Orlovsky GN, Panchin YV, Popova LB, Shupliakov OV. Pharmacologically induced elements of the hunting and feeding behavior in the pteropod mollusk *Clione limacina*. I. Effects of GABA. Journal of Neurophysiology. 1993; 69:512–521. [PubMed: 8459282]

Ascher P. Inhibitory and excitatory effects of dopamine on *Aplysia* neurones. Journal of Physiology. 1972; 225:173–209. [PubMed: 4679683]

Barreiro-Iglesias A, Villar-Cerviño V, Anadón R, Rodicio MC. Dopamine and γ-aminobutyric acid are colocalized in restricted groups of neurons in the sea lamprey brain: insights into the early evolution of neurotransmitter colocalization in vertebrates. Journal of Anatomy. 2009; 215(6):601–610. [PubMed: 19840024]

Benjamin PR, Staras K, Kemenes G. A systems approach to the cellular analysis of associative learning in the pond snail *Lymnaea*. Learning & Memory. 2000; 7:124–131. [PubMed: 10837501]

Berry MS, Cottrell GA. Dopamine: excitatory and inhibitory transmission from a giant dopamine neurone. Nature New Biology. 1973; 242:250–253. [PubMed: 4349780]

Borisovska M, Bensen AL, Chong G, Westbrook GL. Distinct modes of dopamine and GABA release in a dual transmitter neuron. Journal of Neuroscience. 2013; 33(5):1790–1796. [PubMed: 23365218]

Chiang PK, Bourgeois JG, Bueding E. 5-Hydroxytryptamine and dopamine in *Biomphalaria glabrata*. Journal of Parasitology. 1974; 60:264–271. [PubMed: 4821112]

Cooke I, Gelperin A. Distribution of GABA-like immunoreactive neurons in the slug *Limax maximus*. Cell and Tissue Research. 1988; 253:77–81. [PubMed: 2458189]

Cottrell GA. Identified amine-containing neurones and their synaptic connexions. Neuroscience. 1977; 2:1–18. [PubMed: 72363]

Croll, RP. Identified neurons and cellular homologies. In: Ali, M., editor. Nervous Systems in Invertebrates. New York: Plenum Publishing Corp; 1987. p. 41-59.

*This article is derived from the Subject Data funded in whole or part by NAS and USAID. Any opinions, findings, conclusions, or recommendations expressed are those of the authors alone, and do not necessarily reflect the views of USAID or NAS.

Croll RP. Catecholamine-containing cells in the central nervous system and periphery of *Aplysia californica*. Journal of Comparative Neurology. 2001; 441:91–105. [PubMed: 11745637]

Croll RP, Voronezhskaya EE, Hiripi L, Elekes K. Development of catecholaminergic neurons in the pond snail, *Lymnaea stagnalis*: II.Postembryonic development of dopamine-containing neurons and dopamine-dependent behaviors. Journal of Comparative Neurology. 1999; 15:297–309.

de Rijk EP, van Strien FJ, Roubos EW. Demonstration of coexisting catecholamine (dopamine), amino acid (GABA), and peptide (NPY) involved in inhibition of melanotrope cell activity in *Xenopus laevis*: A quantitative ultrastructural, freeze-substitution immunocytochemical study. Journal of Neuroscience. 1992; 12:864–871. [PubMed: 1312137]

Delgado N, Vallejo D, Miller MW. Localization of serotonin in the nervous system of *Biomphalaria glabrata*, an intermediate host for schistosomiasis. Journal of Comparative Neurology. 2012; 520:3236–3255. [PubMed: 22434538]

Dembrow NC, Jing J, Proekt A, Romero A, Vilim FS, Cropper EC, Weiss KR. A newly identified buccal interneuron initiates and modulates feeding motor programs in *Aplysia*. Journal of Neurophysiology. 2003; 90:2190–2204. [PubMed: 12801904]

Díaz-Ríos M, Miller MW. Rapid dopaminergic signaling by interneurons that contain markers for catecholamines and GABA in the feeding circuitry of *Aplysia*. Journal of Neurophysiology. 2005; 93:2142–2156. [PubMed: 15537820]

Díaz-Ríos M, Miller MW. Target-specific regulation of synaptic efficacy in the feeding central pattern generator of *Aplysia*: Potential substrates for behavioral plasticity? Biological Bulletin. 2006; 210:215–229. [PubMed: 16801496]

Díaz-Ríos M, Oyola E, Miller MW. Colocalization of γ-aminobutyric acid-like immunoreactivity and catecholamines in the feeding network of *Aplysia californica*. Journal of Comparative Neurology. 2002; 445:29–46. [PubMed: 11891652]

Dolezalova H, Giacobini E, Stepita-Klauco M. An attempt to identify putative neurotransmitter molecules in the central nervous system of the snail. International Journal of Neuroscience. 1973; 5:53–59. [PubMed: 4144628]

Due MR, Jing J, Weiss KR. Dopaminergic contributions to modulatory functions of a dual-transmitter interneuron in *Aplysia*. Neuroscience Letters. 2004; 358:53–57. [PubMed: 15016433]

Elliott CJ, Benjamin PR. Interactions of the slow oscillator interneuron with feeding pattern-generating interneurons in *Lymnaea stagnalis*. Journal of Neurophysiology. 1985; 54:1412–1421. [PubMed: 4087041]

Elliott CJ, Susswein AJ. Comparative neuroethology of feeding control in molluscs. Journal of Experimental Biology. 2002; 205:877–896. [PubMed: 11916985]

Gerschenfeld HM, Tauc L. Pharmacological specificities of neurons in an elementary nervous system. Nature. 1961; 189:924–925. [PubMed: 13704733]

Goldstein RS, Schwartz JH. Catecholamine neurons in *Aplysia*: improved light-microscopic resolution and ultastructural study using paraformaldehyde and glutaraldehyde (FaGlu) cytochemistry. Journal of Neurobiology. 1989; 20:203–218. [PubMed: 2502605]

Gunaratne CA, Sakurai A, Katz PS. Comparative mapping of GABA-immunoreactive neurons in the central nervous systems of nudibranch molluscs. Journal of Comparative Neurology. 2014; 522:794–810. [PubMed: 24638845]

Gunaratne CA, Katz PS. Comparative mapping of GABA-immunoreactive neurons in the buccal ganglia of nudipleura molluscs. Journal of Comparative Neurology. 2016; 534:1181–1192.

Gutiérrez, R. Co-Existence and Co-Release of Classical Neurotransmitters. New York: Springer Science; 2009.

Habib MR, Mohamed A, Osman GY, Sharaf El-Din A, Mossalem H, Delgado N, Torres G, Rolón-Martínez S, Miller MW, Croll RP. Histamine immunoreactive elements in the central and peripheral nervous systems of the snail, *Biomphalaria* spp., intermediate host for *Schistosoma mansoni*. PLoS ONE. 2015; 10(6):e0129800. http://doi.org/10.1371/journal.pone.0129800. [PubMed: 26086611]

Hatakeyama D, Ito E. Distribution and developmental changes in GABA-like immunoreactive neurons in the central nervous system of the snail, *Lymnaea stagnalis*. Journal of Comparative Neurology. 2000; 418:310–322. [PubMed: 10701829]

Hernádi L. Distribution and anatomy of GABA-like immunoreactive neurons in the central and peripheral nervous system of the snail *Helix pomatia*. Cell and Tissue Research. 1994; 277:189–198. [PubMed: 7914472]

Hirasawa H, Contini M, Raviola E. Extrasynaptic release of GABA and dopamine by retinal dopaminergic neurons. Philosophical Transactions of the Royal Society B. 2015; 370:20140186.

Hirasawa H, Puopolo M, Raviola E. Extrasynaptic release of GABA by retinal dopaminergic neurons extrasynaptic release of GABA by retinal dopaminergic neurons. Journal of Neurophysiology. 2009; 7:146–158.

Hurwitz I, Kupfermann I, Susswein AJ. Different roles of neurons B63 and B34 that are active during the protraction phase of buccal motor programs in *Aplysia californica*. Journal of Neurophysiology. 1997; 78:1305–1319. [PubMed: 9310422]

Ito I, Kimura T, Watanabe S, Kirino Y, Ito E. Modulation of two oscillatory networks in the peripheral olfactory system by gamma-aminobutyric acid, glutamate, and acetylcholine in the terrestrial slug *Limax marginatus*. Journal of Neurobiology. 2004; 59:304–318. [PubMed: 15146547]

Jing J, Vilim FS, Wu JS, Park JH, Weiss KR. Concerted GABAergic actions of *Aplysia* feeding interneurons in motor program specification. Journal of Neuroscience. 2003; 23:5283–5294. [PubMed: 12832553]

Kabotyanski EA, Baxter DA, Byrne JH. Identification and characterization of catecholaminergic neuron B65, which initiates and modifies patterned activity in the buccal ganglia of *Aplysia*. Journal of Neurophysiology. 1998; 79:605–621. [PubMed: 9463425]

Kandel, ER. Behavioral biology of Aplysia: A contribution to the comparative study of opisthobranch molluscs. San Francisco: Freeman Press; 1979.

Katz PS, Harris-Warrick RM. The evolution of neural circuits underlying species-specific behavior. Current Opinion in Neurobiology. 1999; 9:628–633. [PubMed: 10508740]

Kim JI, Ganesan S, Luo SX, Wu YW, Park E, et al. Aldehyde dehydrogenase 1a1 mediates a GABA synthesis pathway in midbrain dopaminergic neurons. Science. 2015; 350:102–106. [PubMed: 26430123]

Kupfermann I. Feeding behavior in *Aplysia*: a simple system for the study of motivation. Behavioral Biology. 1974; 10:1–26. [PubMed: 4815142]

Liu S, Plachez C, Shao Z, Puche A, Shipley MT. Olfactory bulb short axon cell release of GABA and dopamine produces a temporally biphasic inhibition-excitation response in external tufted cells. Journal of Neuroscience. 2013; 33:2916–2926. [PubMed: 23407950]

Maher BJ, Westbrook GL. Co-transmission of dopamine and GABA in periglomerular cells. Journal of Neurophysiology. 2008; 99(3):1559–1564. [PubMed: 18216231]

Mansour TA, Habib MR, Rodríguez LCV, Vázquez AH, Alers JM, Ghezzi A, Croll RP, Brown CT, Miller MW. Central nervous system transcriptome of *Biomphalaria alexandrina*, an intermediate host for schistosomiasis. BioMed Central Research Notes. 2017; 10:729. [PubMed: 29228974]

McCaman MW, Ono JK, McCaman RE. Dopamine measurements in molluscan ganglia and neurons using a new, sensitive assay. Journal of Neurochemistry. 1979; 32:1111–1113. [PubMed: 430045]

Miller, MW. Colocalization and cotransmission of classical neurotransmitters: An invertebrate perspective. In: Gutierrez, R., editor. Co-existence and Co-release of Classical Neurotransmitters. Springer-Verlag; New York: 2008. p. 181-201.

Murphy AD. The neuronal basis of feeding in the snail, *Helisoma*, with comparisons to selected gastropods. Progress in Neurobiology. 2001; 63:383–408. [PubMed: 11163684]

Narusuye K, Kinugawa A, Nagahama T. Responses of cerebral GABA-containing CBM neuron to taste stimulation with seaweed extracts in *Aplysia kurodai*. Journal of Neurobiology. 2005; 65:146–156. [PubMed: 16114014]

Nezlin L, Voronezhskaya E. GABA-immunoreactive neurones and interactions of GABA with serotonin and FMRFamide in a peripheral sensory ganglion of the pond snail *Lymnaea stagnalis*. Brain Research. 1997; 772:217–225. [PubMed: 9406975]

Norekian TP, Malyshev AY. Coordinated excitatory effect of GABAergic interneurons on three feeding motor programs in the mollusk *Clione limacina*. Journal of Neurophysiology. 2005; 93:305–315. [PubMed: 15331621]

Osborne NN, Cottrell GA. Distribution of biogenic amines in the slug, *Limax maximus*. Zeitschrift Fur Zellforschung Und Mikroskopische Anatomie. 1971; 112:15–30. [PubMed: 5544256]

Osborne NN, Briel G, Neuhoff V. Distribution of GABA and other amino acids in different tissues of the gastropod mollusc *Helix pomatia*, including *in vitro* experiments with ^{14}C glucose and ^{14}C glutamic acid. International Journal of Neuroscience. 1971; 1:256–272.

Paul DH. Pedigrees of neurobehavioral circuits: tracing the evolution of novel behaviors by comparing motor patterns, muscles, and neurons in members of related taxa. Brain, Behavior, and Evolution. 1991; 38:226–239.

Rathouz MM, Kirk MD. Localization of catecholamines in the buccal ganglia of *Aplysia californica*. Brain Research. 1988; 458:170–175. [PubMed: 3208096]

Richmond JE, Bulloch AGM, Bauce L, Lukowiak K. Evidence for the presence, synthesis, immunoreactivity, and uptake of GABA in the nervous system of the snail *Helisoma trivolvis*. Journal of Comparative Neurology. 1991; 307(1):131–143. [PubMed: 1856317]

Sakurai A, Katz PS. Phylogenetic and individual variation in gastropod central pattern generators. Journal of Comparative Physiology A: Neuroethology, Sensory, Neural, and Behavioral Physiology. 2015; 201(9):829–839.

Salimova NB, Sakharov DA, Milosevic I, Turpaev TM, Rakic L. Monoamine-containing neurons in the *Aplysia* brain. Brain Research. 1987a; 400:285–299. [PubMed: 3815076]

Salimova NB, Sakharov DA, Milosevic I, Rakic L. Catecholamine-containing neurons in the peripheral nervous system of *Aplysia*. Acta Biologica Hungarica. 1987b; 38:203–212. [PubMed: 3454082]

Seal R, Edwards R. Functional implications of neurotransmitter co-release: glutamate and GABA share the load. Current Opinion in Pharmacology. 2006; 6(1):114–119. [PubMed: 16359920]

Svensson E, Proekt A, Jing J, Weiss KR. PKC-mediated GABAergic enhancement of dopaminergic responses: implication for short-term potentiation at a dual-transmitter synapse. Journal of Neurophysiology. 2014; 112:22–29. [PubMed: 24717352]

Sweeney D. Dopamine: its occurrence in molluscan ganglia. Science. 1963; 139:1051. [PubMed: 13979659]

Teyke T, Rosen SC, Weiss KR, Kupfermann I. Dopaminergic neuron B20 generates rhytmic neuronal activity in the feeding motor circuitry of *Aplysia*. Brain Research. 1993; 630:226–237. [PubMed: 8118689]

Townsend C. The chemorectptor sites involved in food-finding by the freshwater pulmonate snail, *Biomphalaria glabrata* (Say), with particular reference to the function of the tentacles. Behavioral Biology. 1974; 11:511–523. [PubMed: 4416120]

Tritsch NX, Ding JB, Sabatini BL. Dopaminergic neurons inhibit striatal output through non-canonical release of GABA. Nature. 2012; 490:262–266. [PubMed: 23034651]

Tritsch NX, Granger AJ, Sabatini BL. Mechanisms and functions of GABA co-release. Nature Reviews Neuroscience. 2016; 17(3):139–145. [PubMed: 26865019]

Tritt SH, Lowe IP, Byrne JH. A modification of the glyoxylic acid induced histofluorescence technique for demonstration of catecholamines and serotonin in tissues of *Aplysia californica*. Brain Research. 1983; 259:159–162. [PubMed: 6824930]

Trudeau LE, Gutiérrez R. On cotransmission & neurotransmitter phenotype plasticity. Molecular Interventions. 2007; 7:138–146. [PubMed: 17609520]

Trudeau LE, Hnasko T, Wallén-Mackenzie A, Morales M, Rayport S, Sulzer D. The multilingual nature of dopamine neurons. Progress in Brain Research. 2014; 211:141–164. [PubMed: 24968779]

Turner JD, Cottrell GA. Cellular accumulation of amines and amino acids in the central ganglia of a gastropod mollusc, *Planorbis corneus*: an autoradiographic study. Journal of Neurocytology. 1978; 7:759–776. [PubMed: 310450]

Vaaga CE, Borisovska M, Westbrook GL. Dual-transmitter neurons: Functional implications of co-release and co-transmission. Current Opinion in Neurobiology. 2014; 29:25–32. [PubMed: 24816154]

Vaaga CE, Yorgason JT, Williams JT, Westbrook GL. Presynaptic gain control by endogenous cotransmission of dopamine and GABA in the olfactory bulb. Journal of Neurophysiology. 2017; 117:1163–1170. [PubMed: 28031402]

Vallejo D, Habib MR, Delgado N, Vaasjo LO, Croll RP, Miller MW. Localization of tyrosine hydroxylase-like immunoreactivity in the nervous systems of *Biomphalaria glabrata* and *Biomphalaria alexandrina*, intermediate hosts for schistosomiasis. Journal of Comparative Neurology. 2014; 522(11):2532–2552. [PubMed: 24477836]

Walker RJ, Crossman AR, Woodruff GN, Kerkut GA. The effect of bicuculline on the gamma-aminobutyric acid (GABA) receptors of neurones of *Periplaneta* and *Helix aspersa*. Brain Res. 1971; 34:75–82.

Walker RJ, Aranza MJ, Kerkut GA, Woodruff GN. The action of gamma-aminobutyric acid (GABA) and related compounds on two identifiable neurones in the brain of the snail *Helix aspersa*. Comparative Biochemistry and Physiology. 1975; 50C:147–154.

Wentzell MM, Martínez-Rubio C, Miller MW, Murphy AD. Comparative neurobiology of feeding in the opisthobranch sea slug, *Aplysia*, and the pulmonate snail, *Helisoma*: Evolutionary considerations. Brain, Behavior and Evolution. 2009; 74:219–230.

Wu JS, Jing J, Díaz-Ríos M, Miller MW, Kupfermann I, Weiss KR. Identification of a GABA-containing cerebral-buccal interneuron-11 in *Aplysia californica*. Neuroscience Letters. 2003; 341(1):5–8. [PubMed: 12676330]

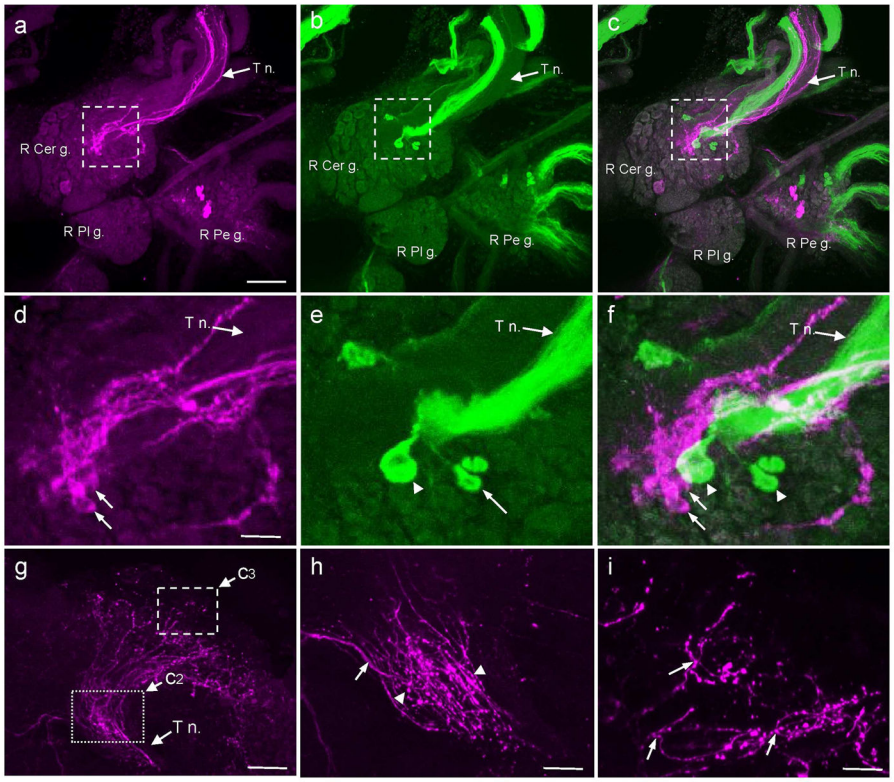

Fig. 1. Comparison of GABAli and THli on the dorsal surface of the *B. glabrata* cerebral ganglion

a: GABAli on the dorsal surface of the right cerebral ganglion (*R Cer g.*). Image also includes the ventral surface of the right pedal ganglion (*R Pd g.*) and the dorsal surface of the right pleural ganglion (*R Pl g.*). GABAli fibers of varying caliber were present in the tentacular nerve (*T n.*). *Calibration bar* = 100 μm applies to **a–c. b:** THli on the dorsal surface of the right pedal ganglion. A large bundle of THli fibers courses through the center of the T n. **c:** Merge of **a** and **b** shows that the GABAli fibers and the THli bundle occupy distinct regions of the tentacular nerve. *Dashed rectangles* in **a–c** denote regions shown at higher magnification in **d–f**, respectively. **d:** Four to six small GABAli cells were embedded within the neuropil at the origin of the tentacular nerve. *Calibration bar* = 30 μm applies to **d–f. e:** A cluster of small THli neurons (*arrow*) and one larger cell (*arrowhead*) with a projection oriented toward the T n. were also located at the base of the nerve. **f:** Merge of **d** and **e** shows that GABAli and THli are not colocalized in the neurons at the origin of the T n. **g:** In the periphery, the GABAli fibers in the T n. reach the epithelium at the base of the tentacle. Dotted and dashed rectangles indicate the regions shown at higher magnification in **h** and **i**, respectively. *Calibration bar* = 50 μm. **h:** The GABAli fibers divide into smaller bundles and fan out to innervate the skin. Some of the larger caliber fibers are smooth (*arrow*), while *en passant* swellings are observed in many of the finer fibers (*arrowheads*). *Calibration bar* = 20 μm. **i:** The fibers terminate as varicose fibers in the skin at the base of the tentacle. *Calibration bar* = 20 μm.

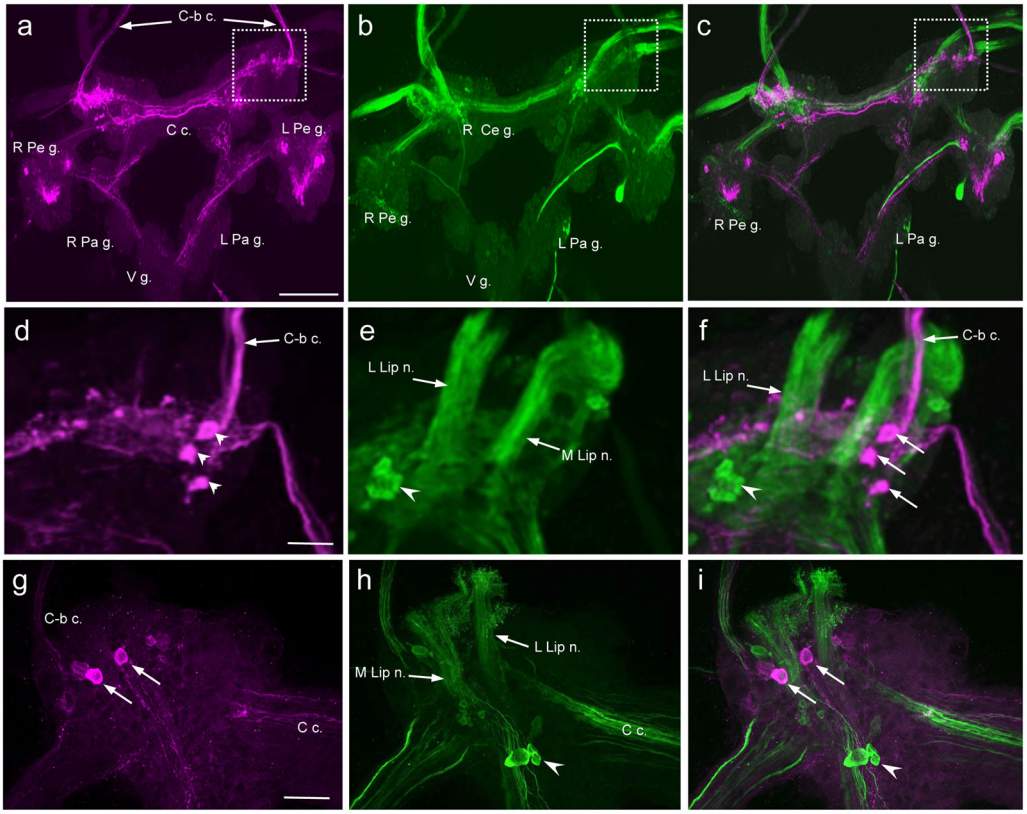

Fig. 2. Comparison of GABAli and THli on the ventral surface of the *B. glabrata* cerebral ganglion

a: GABAli on the ventral surface of the cerebral ganglion. The pedal commissure was severed and the left and right pedal ganglia (*L Pd g.*, *R Pd g.*) were reflected to expose the cerebral ganglion. The ventral surfaces of the remaining subesophageal ganglia are viewed, including the left parietal ganglion (*L Pa g.*), the right parietal ganglion (*R Pa g.*), and the visceral ganglion (*V g.*). GABAli fibers were present in the cerebral commissure (*C c.*) and in the cerebral-buccal connective (*C-b c.*). A dense GABAli neuropil was located in the anterolateral region of each hemiganglion, near the origin of the C-b c. *Calibration bar* = 200 μm applies to **a–c. b:** TH-like immunoreactivity; same view as panel **a**. As with GABAli, THli is most prominent in the anterolateral quadrant of the cerebral ganglion. Major fiber tracts are present in the C c. and in the nerves projecting to the periphery. **c:** Merge of **a** and **b**. Dashed boxes in **a–c** denote region shown at higher magnification in **d–f. d:** GABAli in the anterolateral quadrant of the left cerebral ganglion. Two small cells (*arrowheads*) and one larger soma (*arrow*) are located near the origin of the C-b c. *Calibration bar* = 50 μm applies to **d–f. e:** THli fibers are prominent in the lateral lip nerve (*L Lip n.*) and in the medial lip nerve (*M Lip n.*). A cluster of small THli neurons is located close to the origin of the lateral lip nerve (*L lip n.*). **f:** Merge of **d** and **e**. Colocalization of GABAli and THli was not detected. **g:** GABAli in the anterolateral quadrant of the right cerebral ganglion. Two GABAli cells (*arrows*) are located near the origin of the C-b c. *Calibration bar* = 50 μm applies to **g–i. h:** THli fibers are prominent in the lateral lip nerve (*L Lip n.*) and in the medial lip nerve (*M Lip n.*). A cluster of THli neurons is located close to the origin of the

lateral lip nerve (*arrowhead*). **i:** Merge of **g** and **h.** GABAli and THli colocalization was not detected.

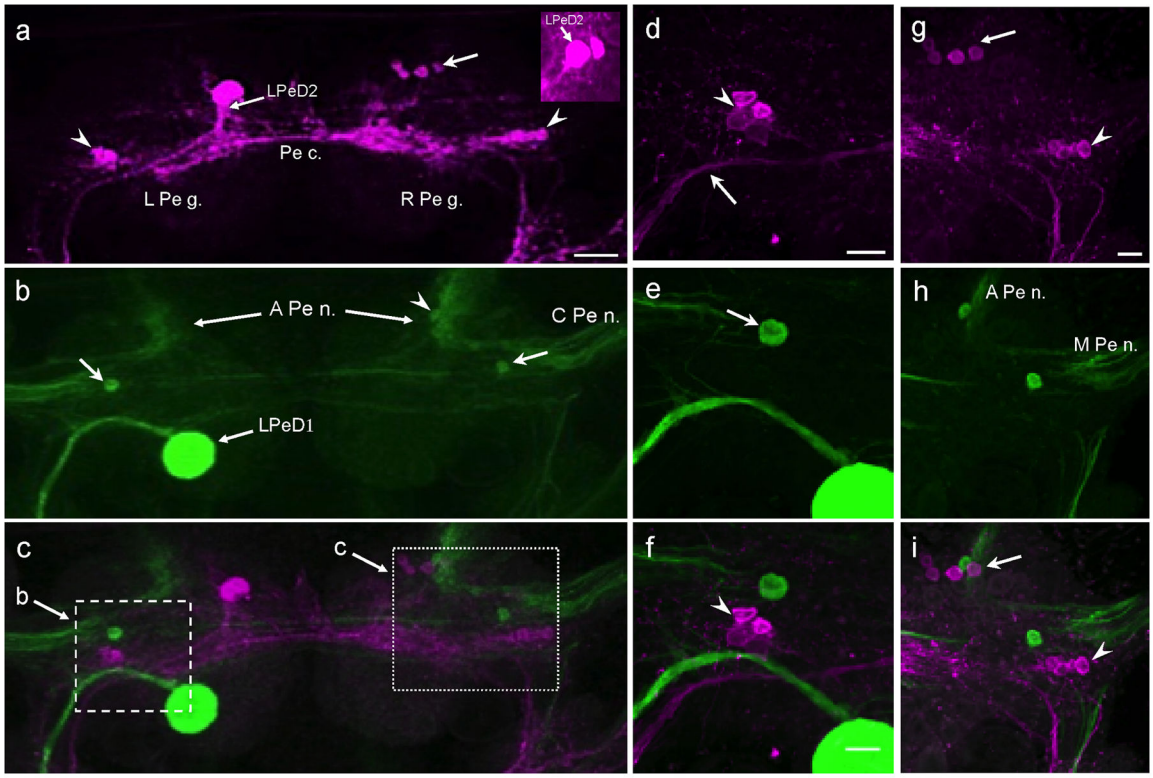

Fig. 3. Comparison of GABAli and THli on the dorsal surface of the pedal ganglion

a: A bilateral cluster of small (10 – 15 μm) neurons (*arrowheads*) was located in the lateral region of each pedal ganglion. While a second anteromedial cluster (*arrow*) was present in the right pedal ganglion (*R Pe g.*) near the origin of the anterior pedal nerve (*A Pe n.*), the left pedal ganglion (*L Pe g.*) contained a large (25 – 30 μm) unpaired neuron (labeled LPeD2) in a comparable position. A stout fiber projected from LPeD2 toward the pedal-pleural connective. A second small immunoreactive cell was often obscured by LPeD2 (inset from another preparation. **b**: THli in the same preparation as **a.** The unpaired giant LPeD1 neuron projects a large axon toward the left pedal-pleural connective. A solitary immunoreactive cell (10–15 μm) was located in the central region of each pedal ganglion (*arrows*) and a smaller cell (*arrowhead*) was embedded in the neuropil at the base of the anterior pedal nerve (*A Pe n.*). **c:** Merge of **a** and **b**. Dashed and dotted boxes indicate regions shown at higher magnification in **f** and **I**, respectively. *Calibration bar* = 50 μm applies to **a–c. d:** The lateral cluster of GABAli neurons (*arrowhead*) in the left pedal ganglion was located near the curvature of the LPeD2 axon (*arrow*). **e:** The solitary THli neuron (*arrow*) was located anterior to the curvature of the LPeD1 axon. **f:** Merged image of **d** and **e** shows that the lateral THli neuron is not located within the lateral cluster of GABAli cells. *Calibration bar* = 30 μm applies to **d–f. g:** Higher magnification of the two clusters of GABAli neurons (*arrow*, *arrowhead*) on the dorsal surface of the right pedal ganglion. **h:** Individual THli neurons are also located near the origins of the A Pe n. and the C Pe n. **i:** Merged image of **g** and **h** shows that the dorsal THli immunoreactive neurons are near, but not part of the GABAli clusters. *Calibration bar* = 20 μm applies to **g–i.**

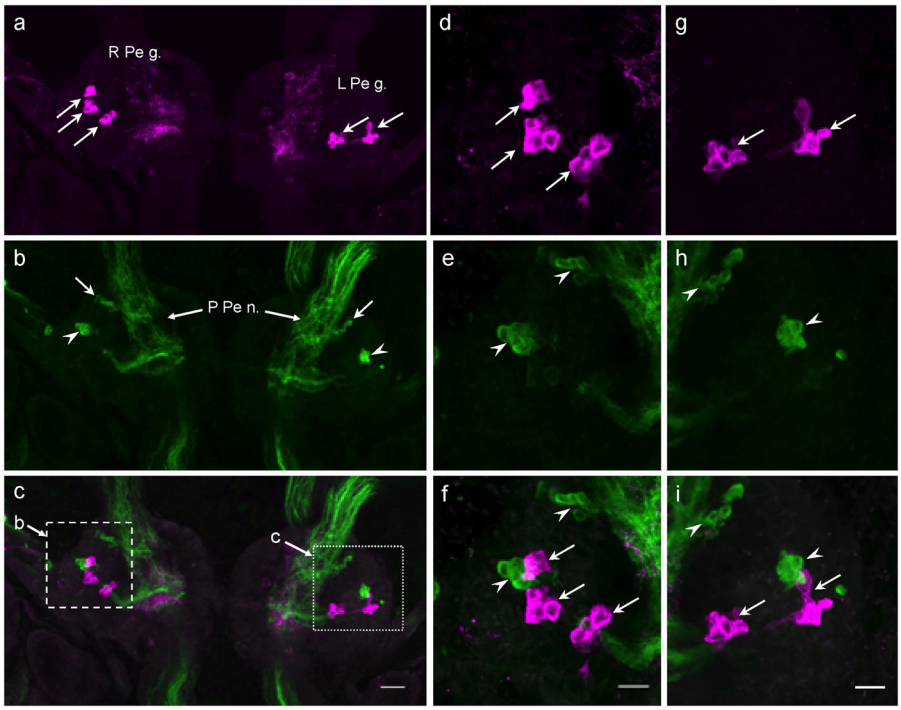

Fig. 4. Comparison of GABAli and THli on the ventral surface of the pedal ganglion

a: Right and left pedal ganglia (*R Pe g.*, *L Pe g.*). Three clusters of four to six small (10–15 μm) GABAli cells (*arrows*) were located in the lateral R Pe g. Two clusters (*arrows*) were located in similar positions in the L Pe g. **b:** THli on the ventral surface of the pedal ganglia; same preparation as a. Two clusters of six to eight small (10–15 μm) cells were present in each pedal ganglion, one near the origin of the posterior pedal nerve (*P Pe n.; arrows*) and another in the anterolateral quadrant (*arrowheads*). **c:** Merged **a** and **b** images show that the lateral GABAli and THli clusters are contiguous. Dashed and dotted rectangles indicate the regions shown at higher magnification in **d–f** and **g–i**, respectively. Calibration bar = 40 μm applies to **a–c. d:** Three clusters of GABAli neurons (*arrows*) on the ventral surface of the right pedal ganglion. **e:** Two clusters of THli neurons (*arrowheads*) on the ventral surface of the right pedal ganglion. **f:** Merge of **d** and **e** shows that the lateral THli and GABAli clusters are contiguous, but the GABAli cluster appears to be more superficial. *Calibration bar* = 20 μm applies to **d–f. g:** Two clusters of GABAli neurons (*arrows*) on the ventral surface of the left pedal ganglion. **h:** Two clusters of THli neurons (*arrowheads*) on the ventral surface of the right pedal ganglion. **i:** Merge of **g** and **h** shows that the lateral THli and GABAli clusters are contiguous, but the THli cluster appears to be more superficial. *Calibration bar* = 20 μm applies to **g–i.**

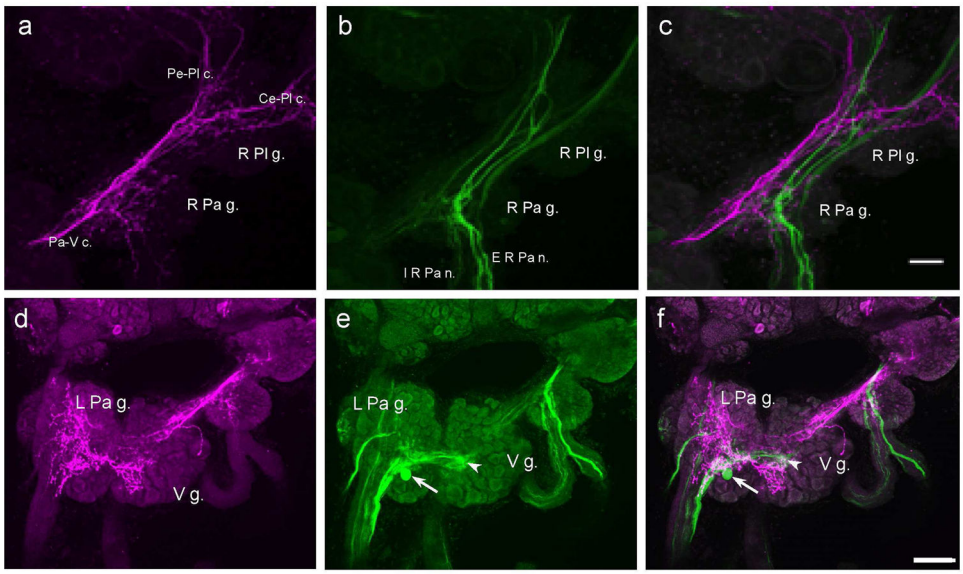

Fig. 5. Comparison of GABAli and THli the pleural, parietal, and visceral ganglia

a: GABAli in the right pleural and right parietal ganglia (*R Pl g.*, *R Pa g.*). Large fibers course through the ganglia, giving rise to extensive central neuropils. The largest fibers could be followed into the pedal-pleural connective (*Pe-Pl c.*), the cerebral-pleural connective (*Ce-Pl c.*) and the parietal-visceral connective (*Pa-V c.*). No immunoreactive cell bodies were detected. **b:** THli in the same preparation. Large fibers course through the R Pl g. and R Pa g. and into the external and internal right parietal nerves (*E R Pa n.*, *I R Pa n.*). **c:** Merge of **a** and **b** panels shows that the GABAli and THli fiber systems are largely segregated into the anterior and posterior regions of the ganglia, respectively. While there is a major projection of THli fibers toward the periphery, the GABAli fibers are confined to the CNS. A few GABAli immunoreactive fibers enter the I R Pa n. but terminate within a short distance. *Calibration bar* = 30 μm applies to **a–c. d:** GABAli in the left parietal ganglion (*L Pa g.*) and visceral ganglion (*V g.*). An extensive network of fibers is present throughout the central neuropil of both ganglia. No GABAli somas were detected and no fibers were present in the peripheral nerves. **e:** THli in the L Pa g. and V g. The arborization of THli is not as extensive as the GABAli neuropil. THli cells are embedded within the neuropil of each ganglion (*arrow*, *arrowhead*; see also Vallejo et al. 2014) and large THli fibers project into the peripheral nerves of the L Pa g. **f:** Merge of **d** and **e** images. No indication of colocalization was observed. *Calibration bar* = 50 μm applies to **d–f.**

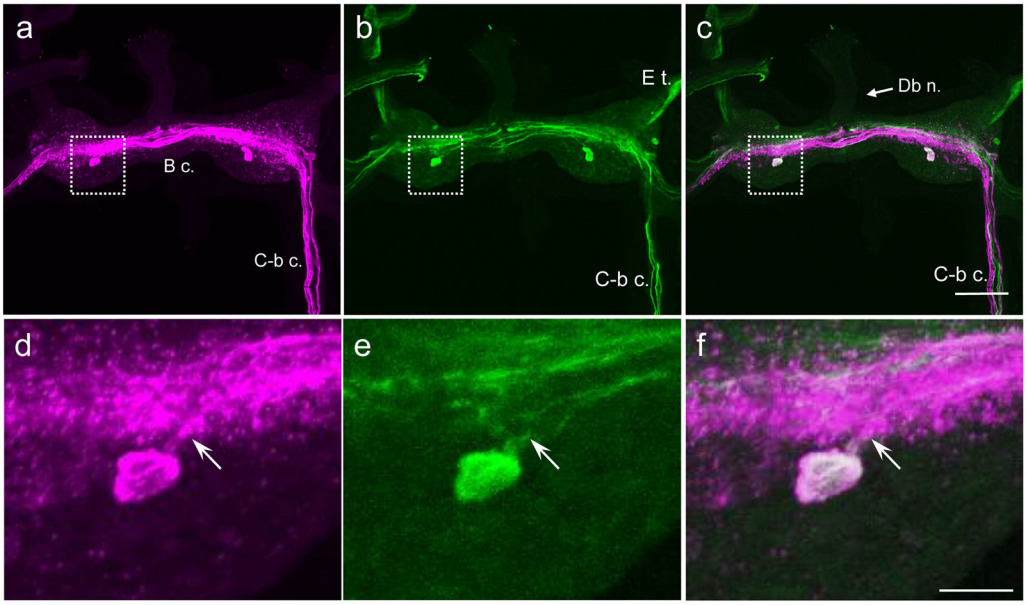

Fig. 6. Comparison of GABAli and THli on the ventral surface of the *B. glabrata* buccal ganglion

a: A prominent system of GABAli fibers courses through the buccal commissure (*B c.*) giving rise to finer networks in the central core of each hemiganglion. Three to five fibers were present in the cerebral-buccal connective (*C-b c.*) and one cell body was located posterior to the central neuropil in each hemiganglion. No GABAli fibers were detected in the buccal nerves. **b:** THli fibers also coursed through the central neuropil of the buccal ganglion. Several fibers were present in the esophageal trunk (*E t.*) and in the C-b c. One THli neuron was located posterior to the fiber systems in each hemiganglion. **c:** Merge of images a and b confirmed that GABAli and THli are colocalized in the two ventral cell bodies. Dotted boxes in **a–c** indicate region shown at higher magnification in panels d–f. *Calibration bar* = 100 μm applies to **a–c. d:** Higher magnification of the GABAli neuron on the ventral surface of the right buccal hemiganglion. A process projected in the anteromedial direction toward the central neuropil (*arrow*). **e:** THli in the same field of view as **d. f:** Merge of **d** and **e** confirms colocalization of GABAli and THli in a single ventral neuron. *Calibration bar* = 25 μm applies to **d–f.**

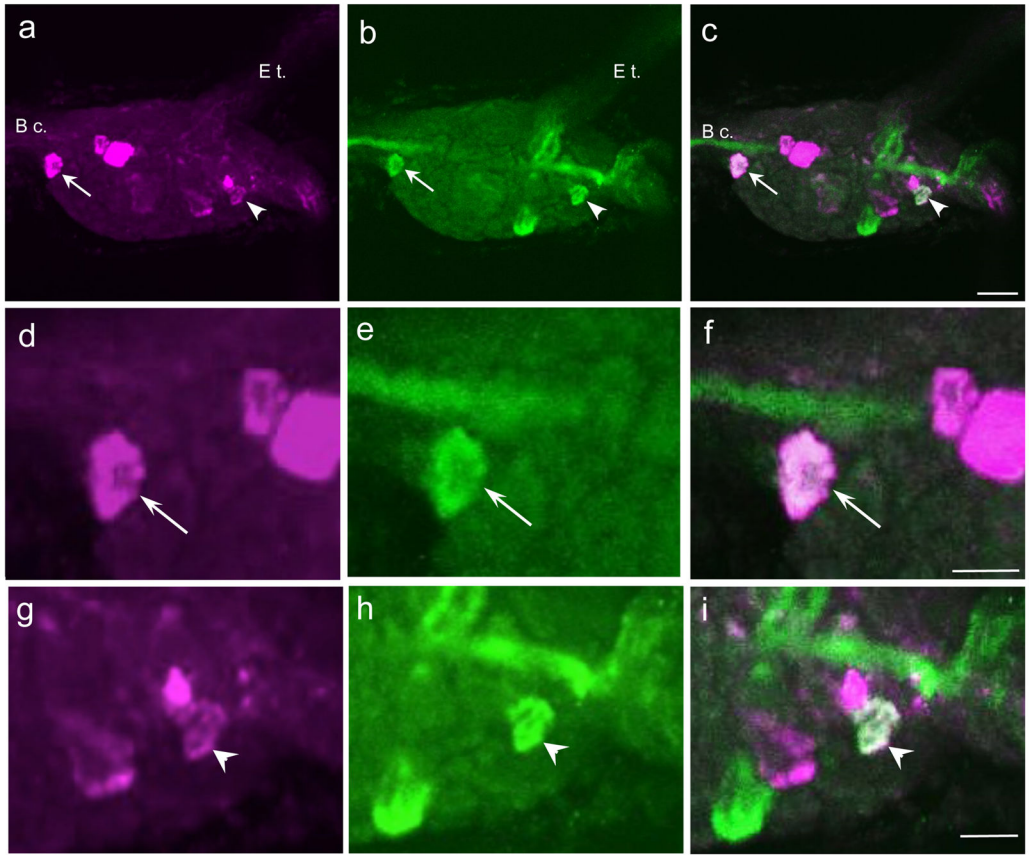

Fig. 7. Comparison of GABAli and THli on the dorsal surface of the *B. glabrata* buccal ganglion

a: Four to six GABAli neurons were present on the dorsal surface of the right hemiganglion. **b:** THli was present in three to five dorsal neurons, including one lateral cell (*arrowhead*) and an unpaired cell near the midline (*arrow*) that appeared to correspond to GABAli neurons. **c:** A merge of **a** and **b** confirmed GABAli-THli colocalization in two dorsal cells. *Calibration bar* = 50 μm applies to **a–c. d:** Higher magnification of the medial GABAli cell shown in **a. e:** THli in the same field as **d. f**: Merge of **d** and **e** confirms GABAli-THli colocalization. Two GABAli cells that do not contain THli are also shown. *Calibration bar* = 25 μm applies to **d–f. g:** Higher magnification of the lateral GABAli cell shown in **a. b:** THli in the same field as **g. i:** Merge of g and h confirms GABAli-THli colocalization. *Calibration bar* = 25 μm applies to **g–i.**

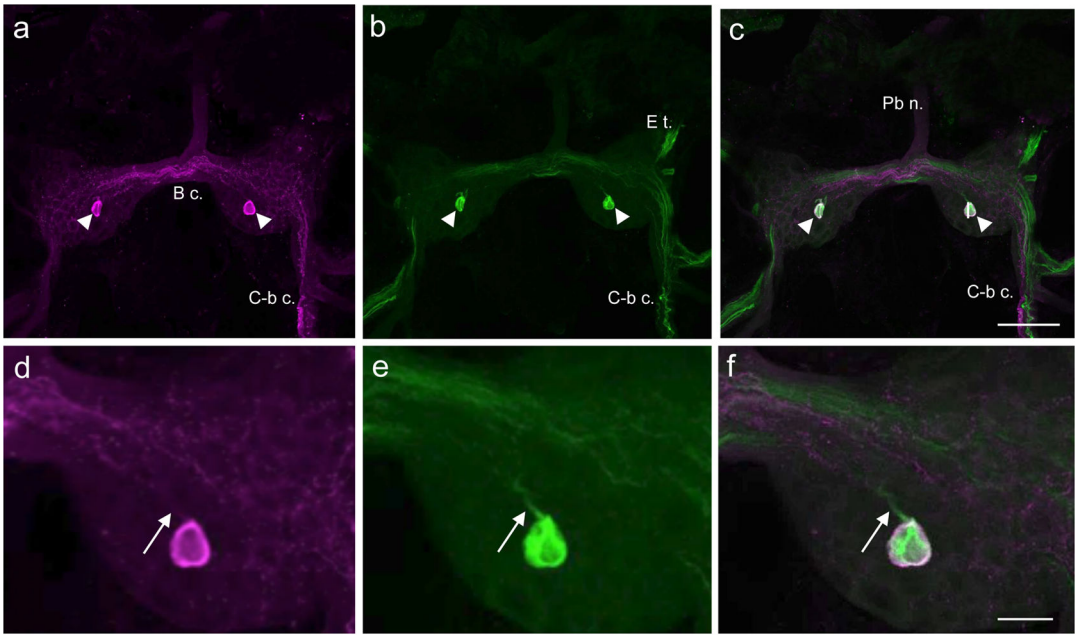

Fig. 8. Comparison of GABAli and THli on the ventral surface of the *Lymnaea stagnalis* buccal ganglion

a: A prominent system of GABAli fibers courses through the buccal commissure (*B c.*) and three to five fibers are present in the cerebral-buccal connective (*C-b c.*). One cell body was located posterior to the central neuropil in each hemiganglion (*arrowheads*). No GABAli fibers were detected in the buccal nerves. **b:** THli fibers also coursed through the central neuropil of buccal ganglion. Several fibers were present in the esophageal trunk (*E t.*) and in the C-b c. One THli neuron was located posterior to the fiber systems in each hemiganglion (*arrowheads*). **c:** Merge of images **a** and **b** confirmed that GABAli and THli are colocalized in the two ventral cell bodies. *Calibration bar* = 100 μm applies to **a–c. d:** Higher magnification of the GABAli neuron on the ventral surface of the right buccal hemiganglion. A process projected in the anteromedial direction toward the buccal commissure (*arrow*). **e:** THli in the same field of view as **d. f:** Merge of **d** and **e** confirms colocalization of GABAli and THli in a single ventral neuron. *Calibration bar* = 25 μm, applies to **d–f.**

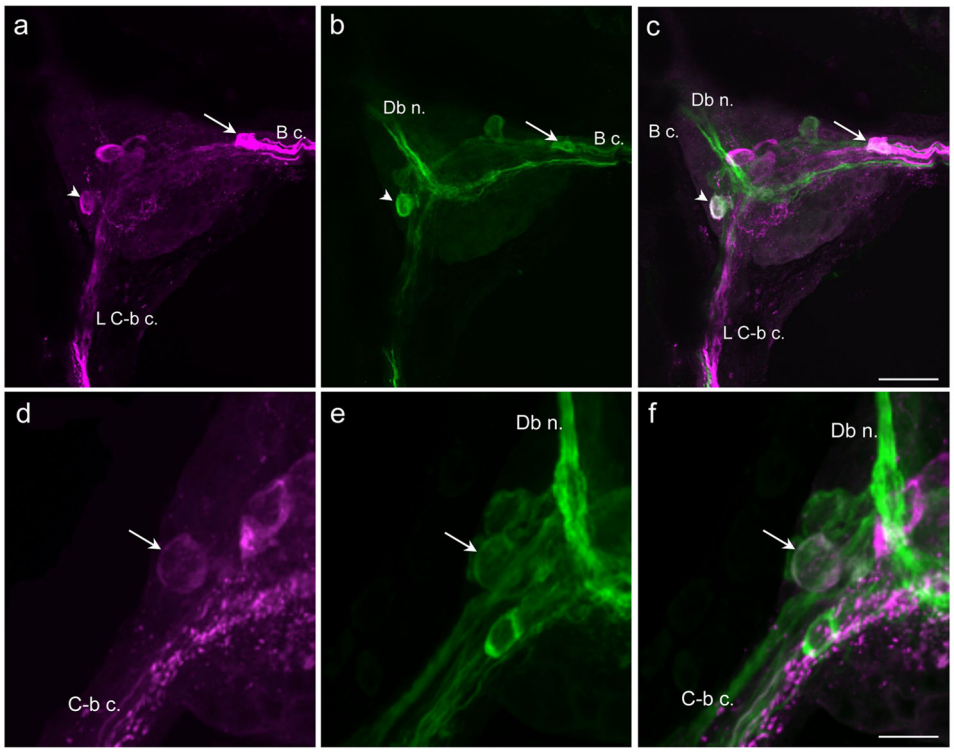

Fig. 9. Comparison of GABAli and THli on the dorsal surface of the *Lymnaea stagnalis* buccal ganglion

a: Four to six GABAli neurons were present on the dorsal surface of the left hemiganglion. **b:** THli was present in three to five dorsal neurons, including one lateral cell (*arrowhead*) and an unpaired cell near the midline (*arrow*) that appeared to correspond to GABAli neurons. **c:** A merge of **a** and **b** confirmed GABAli-THli colocalization in two dorsal cells. *Calibration bar* = 100 μm applies to **a–c. d:** Higher magnification of the lateral GABAli cell shown in **a. e:** THli in the same field as **d. f:** Merge of **d** and **e** confirms GABAli-THli colocalization. GABAli cells that do not contain THli and THli cells that do not contain GABAli are also shown. *Calibration bar* = 25 μm applies to **d–f.**

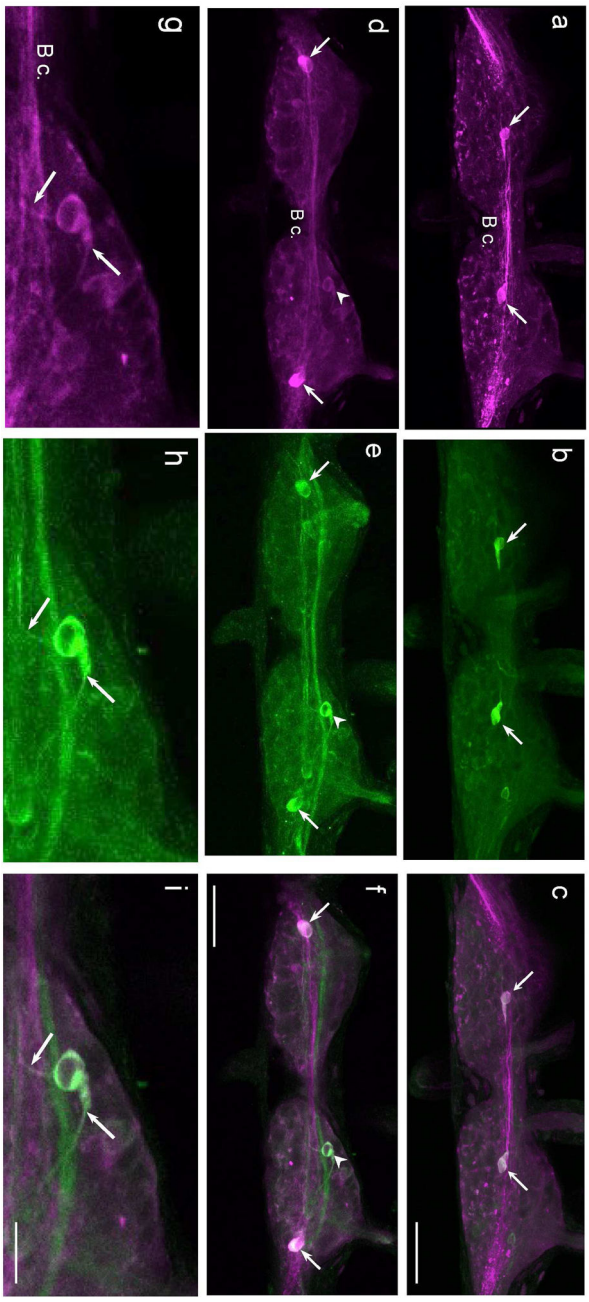

Fig. 10. Comparison of GABAli and THli in the buccal ganglion of *Helisoma trivolvis*

a: A prominent system of GABAli fibers courses through the buccal commissure (*B c.*). One cell body was located slightly posterior to the central neuropil in each hemiganglion (*arrows*). **b:** One THli neuron was located in the medial region of each hemiganglion (*arrows*). **c:** Merge of images **a** and **b** confirmed that GABAli and THli are colocalized in the two ventral cell bodies. *Calibration bar* = 100 μm applies to **a–c. d:** Three to four GABAli cell bodies were observed on the dorsal surface of the *Helisoma* buccal ganglion, including two lateral cells (*arrows*) and one unpaired cell in the right hemiganglion near the B c. (*arrowhead*). A process projected in the anteromedial direction toward the buccal

commissure (*arrow*). **e:** THli in the same field of view as **d. f:** Merge of **d** and **e** confirms colocalization of GABAli and THli in the two lateral cells (*arrows*) and the unpaired cell (*arrowhead*). *Calibration bar* = 100 μm, applies to **d–f. g:** Higher magnification of the unpaired GABAli neuron. Arrows indicate two projections. **h:** Unpaired THli neuron. **i:** Merge of **g** and **h** confirms GABAli-THli colocalization. *Calibration bar* = 30 μm applies to **g–i.**

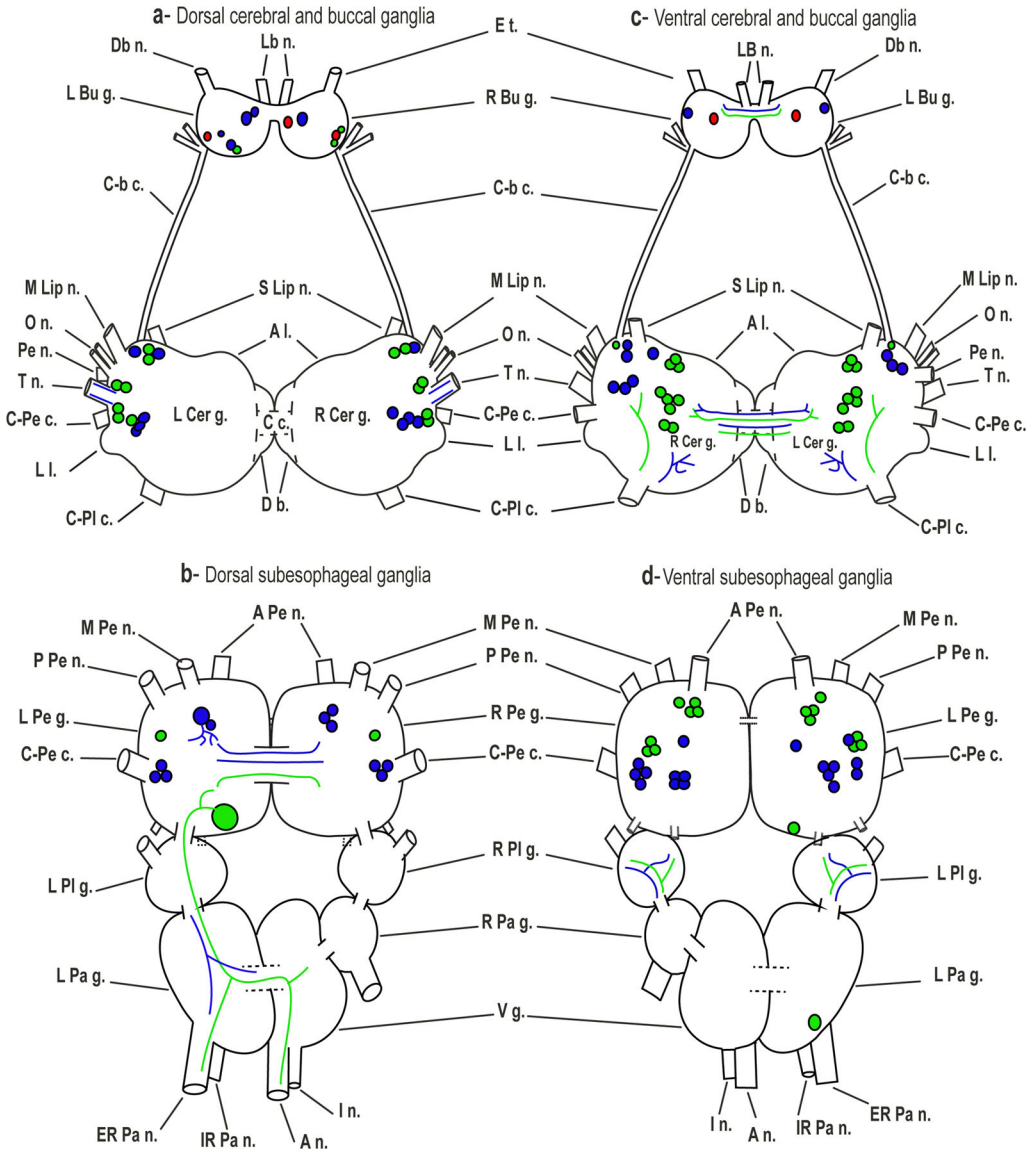

Fig. 11. Schematic summary of GABAli and THli in *Biomphalaria*

GABAli cells and projections (blue) and THli (green) are shown for the dorsal (left panel) and ventral (right panel) central nervous system (applies to *B. glabrata* and *B. alexandrina*). Buccal cells in which GABAli and THli were colocalized are coded red. Abbreviations: A n.: anal nerve, A Pe n.: anterior pedal nerve, C c.: cerebral commissure, C-Pe c.: cerebral-pedal connective, Db n.: dorsobuccal nerve, ER Pa n.: exterior parietal nerve, E t.: esophageal trunk, I n.: intestinal nerve, IR Pa n.: Interior parietal nerve, L Bu g.: left buccal ganglion L Cer g.: left cerebral ganglion, L Pa g.: left parietal ganglion, L Pe g.: left pedal ganglion, L Pl g.: left pleural ganglion, M Lip n.: medial lip nerve, M Pe n.: median pedal nerve, O n.: optic nerve, Pb n.: parabuccal nerve, P n.: penial nerve, P Pe n.: posterior pedal nerve, R Bu g.: right buccal ganglion, R Cer g.: right cerebral ganglion, R Pa g.: right parietal ganglion, R Pd g.: right pedal ganglion, R Pl g.: right pleural ganglion, S Lip n.: superior lip nerve, T n.: tentacular nerve, Vg.: visceral ganglion.